Mode Structure Analysis of Detached Plasmas with 2D Images

Shin KAJITA, Hirohiko TANAKA[1)], Noriyasu OHNO[1)] and Takuya ONDA[1)]

Institute of Materials and Systems for Sustainability, Nagoya University, Nagoya 464-8603, Japan
[1)]Graduate School of Engineering, Nagoya University, Nagoya 464-8603, Japan

(Received 5 September 2017 / Accepted 25 March 2018)

In linear plasma devices, blob-like cross-field transport is enhanced especially in detached plasmas. Formation of blob-like plasmas in the linear plasma device NAGDIS-II was observed using a fast framing camera, and the mode analysis was conducted using the emission from the plasma column. From the Fourier analysis, it was seen that plasma instability was enhanced before the ejection of blob-like plasmas from the plasma column. It was found that blob-like plasmas are generated at the peripheral region of the plasma column associated with low mode number ($m = 0$ - 2) plasma instability inside the plasma column.

Keywords: detached plasma, plasma blob, mode analysis, plasma instability

DOI: 10.1585/pfr.13.1402033

1. Introduction

In fusion devices, divertor materials are subjected to high heat and particle loads. To keep the heat load to the divertor plate less than the safety limit, neutralization of plasmas via radiation from impurity and volumetric plasma recombination processes, so called plasma detachment [1], is thought to be inevitable, and control of plasma detachment is an important issues in next fusion devices. However, there are still issues with the modeling of the plasma detachment; a discrepancy between the experimental results and the numerical simulation regarding the particle flux reduction [2] suggested unknown features in the atomic and molecular processes and/or cross-field transports.

Intermittent cross-field convective plasma transport, so called plasma blob, has been observed in SOL in several magnetically confined plasma devices [3]. Plasma blob has a filamentary structure along the magnetic field line and has a higher density than the SOL plasma. Interestingly, the cross-filed plasma transport, which could be associated with plasma blob-like structure, was found to be enhanced in the detached plasma condition in linear plasma devices [4–6], helical devices [7], and tokamaks [8,9]. In the linear plasma device NAGDIS-II (NAGoya DIvertor plasma Simulator II), fast framing camera observations have revealed that a spiral structure ejected from the plasma column was rotated in $\boldsymbol{E} \times \boldsymbol{B}$ direction in the peripheral region of the plasma column, where the electric field was in the radial direction [4,10]. Recent three dimensional simulation aiming at linear plasma devices predicted that resistive drift instability leads to generation of blob-like structures [11]. From the simulation, it was also suggested that the instability with $m = 0$ mode in the core region of the cylindrical plasma was important for the spiral structure formation in linear devices in addition to the instability with $m = 1$ mode [12]. However, the dynamics in the plasma column especially in the core region has yet to be investigated, because the intensity in the core region was saturated in previous works [4, 10].

In this work, we observed dynamical changes of plasma column accompanied with the generation of blob-like structures in detached plasma of the linear plasma device NAGDIS-II. Using the fast framing camera images, mode analysis of plasma instability inside the plasma column was conducted using the Fourier method. The relation between the spiral structure formation and growth of instability in the plasma column is discussed.

2. Methods

2.1 Experimental

The experiment was performed in the linear divertor plasma simulator NAGDIS-II. Figure 1 (a) shows a schematic of the experimental setup. To observe the dynamic behavior of the plasma, a viewing port (quartz glass) was installed at the end of NAGDIS-II to observe the plasma from a field of view in parallel to the magnetic field. The distance from the anode to the viewing port was 2.0 m. The discharge current was 30 A, and the magnetic field strength was 75 mT. The neutral pressure in the downstream chamber was 14.6 mTorr. A fast framing camera (ULTRA CAM HS-106E: NAC Image Technology, Inc.) was used for the observation. One of advantages of the usage of the fast framing camera is in the fact that full image size observations up to 1.25 M frames/s are possible, though the number of images is limited to 120 frames. It is noted that we can observe the instabilities inside the plasma column in this study by using the framing camera at faster frame rate (100 kfps) compared with the previous study (30 kfps), in which only the ejected spiral structures are analyzed, because the intensity was saturated in the

author's e-mail: kajita.shin@nagoya-u.jp

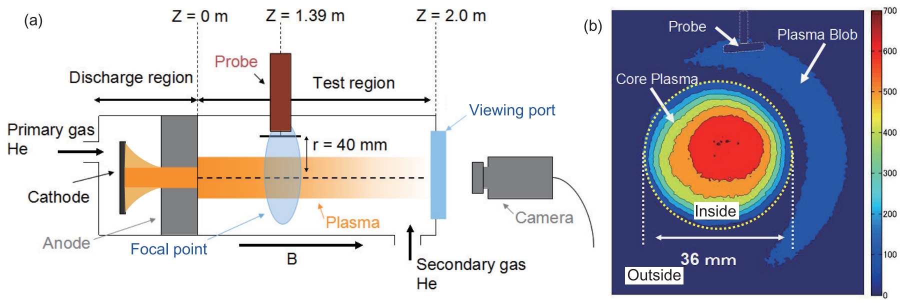

Fig. 1 (a) A schematic of the experimental setup in NAGDIS-II, and (b) a typical image taken by the fast framing camera.

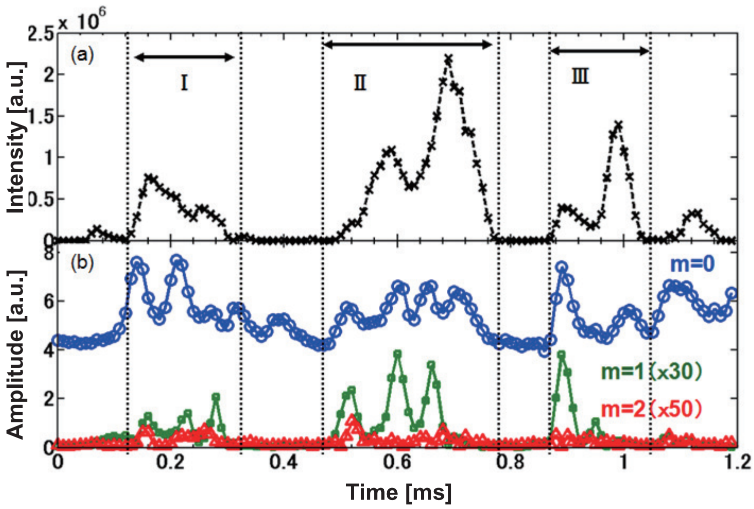

Fig. 2 (a) The temporal evolution of the emission in the peripheral region of the plasma column, and (b) intensity of the modes (m = 0, 1, and 2) of the plasma column structure (r < 36 mm).

core region.

Figure 1 (b) shows a typical image taken by the fast framing camera. In addition to the core part of the plasma, of which the diameter is ∼30 mm, a spiral structure can be identify. The plasma blob in tokamaks is formed by a gradient-driven instability, but the phenomenon observed in our device could be driven by a different mechanism. In this study, we call this structure as plasma blob for convenience hereafter, though the mechanism is not necessarily the same as the plasma blobs in tokamaks.

2.2 Analysis

The mode structure analysis was performed using images taken by the fast framing camera. The overall behavior of modes inside the plasma column were examined by considering averaged amplitudes defined as

$$E_m(t) = \int_0^R |i_m|^2 r\mathrm{d}r, \tag{1}$$

$$i_m(r,t) = \frac{1}{2\pi}\int_0^{2\pi} i(r,\theta,t)\mathrm{e}^{-im\theta}\mathrm{d}\theta. \tag{2}$$

Here, r is the radial distance from the plasma center, θ is the azimuthal angle, and m is the mode number. In Eq. (1), R of 36 mm was used, as shown in Fig. 1 (b). The value $i_m(r,t)$ is the amplitude calculated from the emission intensity, $i(r,\theta,t)$, using the Fourier transform, and $E_m(t)$ is the radially averaged amplitude of m mode at time t.

3. Results and Discussion

Figure 2 (a) shows the temporal evolution of the emission in the peripheral region of the plasma column. The emission intensity outside of the plasma column (r > 36 mm) was integrated. We can identify several peaks in the emission, which corresponds to the appearance of plasma blobs. Major periods of time where strong emission was identified were 0.1 - 0.28 ms (period I), 0.5 - 0.78 ms (period II), and 0.87 - 1.05 ms (period III). We later show the images during the periods of time and discuss the behavior of plasma column in detail.

Figure 2 (b) shows the intensity of the modes (m = 0, 1, and 2) of the plasma column structure (r < 36 mm) analyzed with the Fourier method using Eqs. (1), (2). Here, m = 0, 1, and 2 modes correspond to circular, decentered, and elliptical components, respectively. Because the intensities of m = 1 and 2 were much smaller than that of

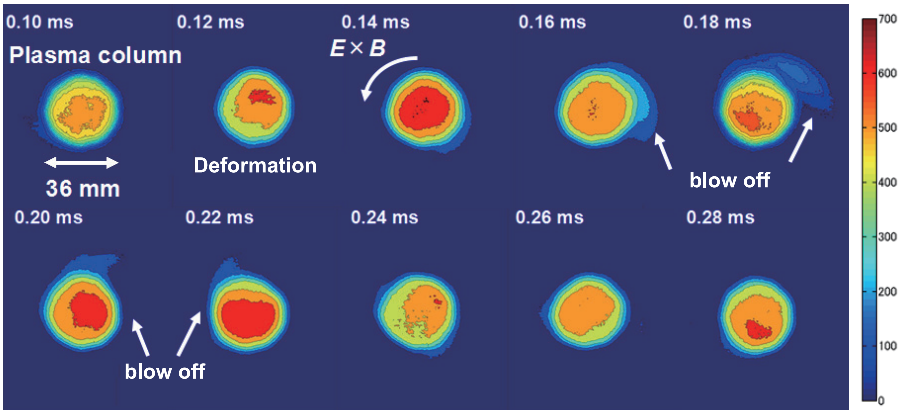

Fig. 3 Consecutive images of the plasma column during period I.

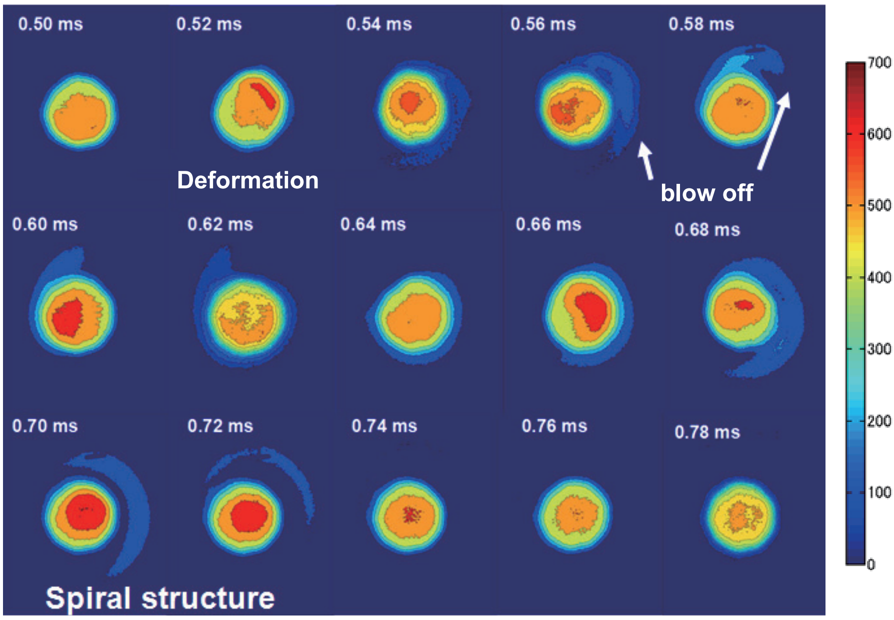

Fig. 4 Consecutive images of the plasma column during period II.

m = 0, the intensities were expanded 30 times for m = 1 and 50 times for m = 2 in Fig. 2 (b). Note that the fluctuation in the temporal evolution is important for m = 0 in particular, because m = 0 modes includes offset from its definition. In periods I - III, major components were m = 0 and 1 modes, and slight increase in m = 2 mode was also observed. When the plasma was stable without any ejection to the peripheral region, the plasma column was composed of only m = 0 structure. The increases in mode 0, 1 and 2 structures were identified at the same timing or just before the increase in the emission from the outside of plasma column.

Figure 3 show consecutive images of the plasma column during period I. It is seen that a blowoff of plasma blob occurred from 0.16 ms while the plasma column rotated in $\boldsymbol{E}_r \times \boldsymbol{B}$ direction, where $\boldsymbol{E}_r$ is the electric field vector in the radial direction. In the NAGDIS-II device, the plasma potential becomes negative in the plasma center, because of Penning ionization gauge (PIG) discharge with a hollow anode structure [13], and the combination of the inward electric field and the magnetic field formed by solenoidal coils determined the $\boldsymbol{E}_r \times \boldsymbol{B}$ direction. We can also identify a deformation of the plasma column at 0.12 ms and an increase in the emission at 0.14 ms, slightly before the plasma blowoff.

During period II, as shown in Fig. 4, blowoffs from the plasma column were observed twice at ~0.56 and 0.68 ms. Similar to period I, deformation was identified at 0.52 and 0.66 ms, slightly before the blowoffs. In period II, it is seen that spiral structure was clearly detached from the plasma column. Recently, laser Thomson scattering in NAGDIS-II revealed that a cold (~0.1 eV) high density plasma existed in the peripheral region in detached plasmas [14]. It is likely that the plasma blowoffs shown in Fig. 4 resulted

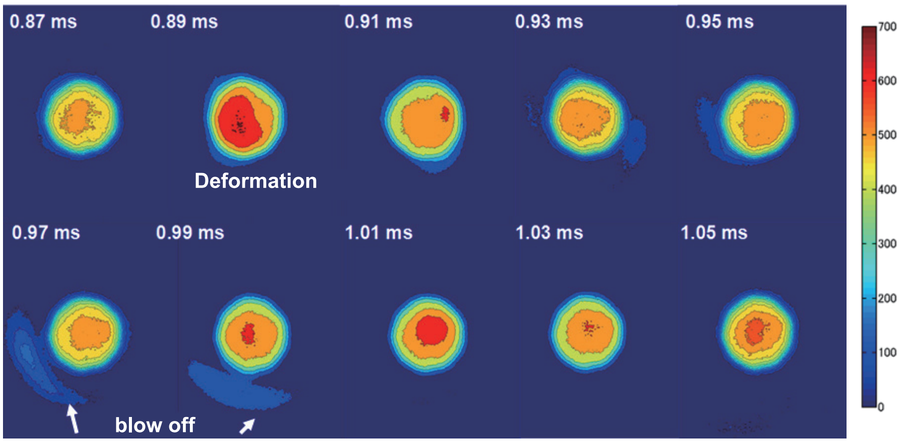

Fig. 5 Consecutive images of the plasma column during period III.

in the formation of the cold plasmas in the peripheral region.

In period III, a blowoff occurred at 0.97 ms, and a deformation of the plasma column occurred at 0.89 ms, as shown in Fig. 5. When the plasma column was deformed, the intensity in the core also increased; this corresponds to the increase in $m = 0$ intensity. After the blowoff, the spiral structure detached from the core was clearly identified. In all the three periods of time, a deformation of plasma column and an increase in the emission intensity occurred slightly before the plasma blowoff.

From Figs. 3 - 5, one can say that plasma column was decentered with a distortion in the shape, and, consequently, $m = 1$ mode grew. In Fig. 2 (b), the variation of $m = 0$ mode was much greater than the other modes. In Figs. 3 - 5, in addition to the above mentioned $m = 1$ mode, the signal intensity inside the column significant altered temporally. The variations in the plasma column size and the intensity, which would be caused by the increases in the density or temperature of the plasma, correspond to the dominant $m = 0$ mode. In other words, one can say that the formation of the plasma blob was originated from the growth of $m = 1$ mode instability accompanied by the growth of $m = 0$ mode instability.

A wavelet analysis [15] was conducted for the time evolution of $m = 1$ mode intensity shown in Fig. 6 (a). Figure 6 (b) shows the temporal evolution of wavelet spectrum. Previously, blob-like phenomena were observed in a similar linear device TPD-Sheet IV [6], where the blowoffs occur periodically. Different from TPD-Sheet IV, the phenomena were intermittent in NAGDIS-II. In this study, the characteristic time scale of the phenomena was in the range of 10 - 20 kHz. Tanaka *et al.* showed under a different condition in NAGDIS-II that the ejection frequency was approximately 3.2 kHz [10], and it was 2.0 kHz in simulation [12]. Although the rotation frequency of blob-like plasma has been revealed to depend on the magnetic field strength and density profile, no detailed investigation has yet to be conducted for the ejection frequency; the results in this study suggested that the ejection frequency also altered by the plasma condition.

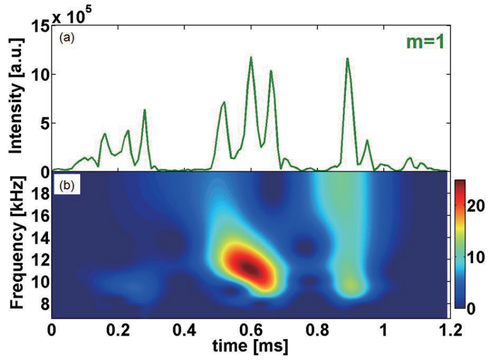

Fig. 6 (a) Time evolution of $m = 1$ mode intensity and (b) time evolution of the wavelet spectrum.

Reiser *et al.* discussed based on three-dimensional global drift fluid dynamics simulation that spiral structures, like the one observed in the NAGDIS-II device, is dominated by $m = 1$ and $m = 2$ modes with a time oscillation of $m = 0$ mode [12]. Thus, the present mode analysis are qualitatively agree well with the global drift fluid dynamic simulation. In the simulation, the temporal evolutions of $m = 0$ and $m = 1$ mode instability were out of phase, indicating that the instability was driven by predator-prey like mechanism. In this study, $m = 0$ and $m = 1$ modes are almost in phase. One of the reasons is attributed to the fact that the analysis in [12] included the peripheral region, while we focused on inside the plasma column in this study. However, even if we included the peripheral region for the analysis, the in phase tendency would not be reduced. One of the potential reasons to cause the discrepancy was a line integrated effect in the measurement. Also, the mechanisms to produce blobs could be different between the experiments and simulation. It remained for our future work to investigate the phenomena using a local measurement such as an electrostatic probe. Further detailed experimental investigation with comparison with simulation is current underway using a multi-electrode target plate, which enables local fluctuation analysis.

4. Conclusions

Images taken by a fast framing camera from axial field of view in the linear plasma device NAGDIS-II were analyzed in the detached plasma condition. Plasma blowoff from the periphery of the plasma column was observed while the plasma rotated azimuthally in $\boldsymbol{E}_r \times \boldsymbol{B}$ direction. Spiral shaped plasma blobs were formed accompanied with the blowoffs. The Fourier mode analysis of the instability in the plasma column shows that low mode instability ($m = 0$, 1, and 2) was grown at the same timing of just before the plasma ejection occurred. The present study supported the drift fluid dynamics simulation for the formation of spiral structure formation in linear plasma devices [12]. At the moment, $m = 1$ mode and $m = 0$ mode instabilities grew in-phase and the predator-prey like mechanism discussed based on the simulation was not observed experimentally; we are planning further investigations based on local measurements in future.

Acknowledgments

This work was supported in part by a Grant-in Aid for Scientific Research 25289337, 25610170, 15H04229, and 16H06139 from the Japan Society for the Promotion of Science (JSPS). It was also supported in part by NIFS/NINS under the project of Formation of International Network for Scientific Collaborations and NIFS Collaboration Research Program (NIFS15KOAH032, NIFS17KUGM120).

[1] S.I. Krasheninnikov, A.S. Kukushkin and A.A. Pshenov, Phys. Plasmas **23**, 055602 (2016).
[2] K. Hoshino, K. Shimizu, T. Takizuka, N. Asakura and T. Nakano, J. Plasma Fusion Res. Series **9**, 592 (2010).
[3] G.Y. Antar, G. Counsell, Y. Yu, B. Labombard and P. Devynck, Phys. Plasmas **10**, 419 (2003).
[4] H. Tanaka, N. Ohno, Y. Tsuji and S. Kajita, Contrib. Plasma Phys. **50**, 256 (2010).
[5] E.M. Hollmann, C. Brandt, B. Hudson, D. Kumar, D. Nishijima and A.Y. Pigarov, Phys. Plasmas **20**, 093303 (2013).
[6] T. Onda, S. Kajita, T. Iijima, A. Tonegawa, N. Ohno and H. Tanaka, Contrib. Plasma Phys. **57**, 87 (2017).
[7] H. Tanaka, N. Ohno, Y. Tsuji, S. Kajita, S. Masuzaki, M. Kobayashi, T. Morisaki, H. Tsuchiya, A. Komori and L.E. Group, Phys. Plasmas **17**, 102509 (2010).
[8] B. Stansfield *et al.*, J. Nucl. Mater. **241**, 739 (1997).
[9] S. Potzel, M. Wischmeier, M. Bernert, R. Dux, H. Muller and A. Scarabosio, J. Nucl. Mater. **438**, S285 (2013), proceedings of the 20th International Conference on Plasma-Surface Interactions in Controlled Fusion Devices.
[10] H. Tanaka, N. Ohno, Y. Tsuji, K. Okazaki and S. Kajita, Contrib. Plasma Phys. **52**, 424 (2012).
[11] D. Reiser, Phys. Plasmas **19**, 072317 (2012).
[12] D. Reiser, N. Ohno, H. Tanaka and L. Vela, Phys. Plasmas **21**, 032302 (2014).
[13] N. Ohno, D. Nishijima, S. Takamura, Y. Uesugi, M. Motoyama, N. Hattori, H. Arakawa, N. Ezumia, S. Krasheninnikov, A. Pigarov and U. Wenzel, Nucl. Fusion **41**, 1055 (2001).
[14] S. Kajita *et al.*, Phys. Plasmas **24**, 073301 (2017).
[15] N. Ohno, V. Budaev, K. Furuta, H. Miyoshi and S. Takamura, Contrib. Plasma Phys. **44**, 222 (2004).